Engineering Science and Technology, an International Journal 23 (2020) 1223–1232

HOSTED BY

Contents lists available at ScienceDirect

Engineering Science and Technology, an International Journal

journal homepage: www.elsevier.com/locate/jestch

Full Length Article

Testing and modelling the fatigue behaviour of GFRP composites – Effect of stress level, stress concentration and frequency

Wahid Ferdous [a,*], Allan Manalo [a], Joshua Peauril [a], Choman Salih [a], Kakarla Raghava Reddy [a], Peng Yu [a], Peter Schubel [a], Tom Heyer [b]

[a] University of Southern Queensland, Centre for Future Materials (CFM), Toowoomba, QLD 4350, Australia
[b] Austrak Pty. Ltd., Brisbane, QLD 4001, Australia

ARTICLE INFO

Article history:
Received 23 September 2019
Revised 22 December 2019
Accepted 7 January 2020
Available online 28 January 2020

Keywords:
Glass fibres
Stress concentration
Failure theory
Analytical model

ABSTRACT

The effects of stress level, stress concentration and frequency on the fatigue life of glass fibre reinforced polymer (GFRP) composites have been investigated under tension-tension fatigue at a stress ratio of 0.1. Vinyl ester-based GFRP laminates were tested at a stress level of 80%, 70%, 60%, 50%, 40% and 25% of the ultimate tensile strength until the failure or up to 8 million cycles whichever comes first in order to determine fatigue life and identify failure modes. The results showed that the composites failed in pure tension at high applied stress while the failure was dominated by stress concentration at low stress level. Moreover, stress concentration was found to reduce the fatigue life of the laminated composites and the test frequency of up to 8 Hz did not induce excessive self-heating. The mean stress failure criteria was found appropriate for numerical modelling of GFRP composites subjected to low level of stress while Goodman failure criteria is suitable at high stress condition. The analytical model considering the effect of stress ratio, applied maximum stress, frequency and material properties is able to predict reliably the fatigue life of GFRP composites in tension.

1. Introduction

The acceptance and application of fibre reinforced polymer (FRP) composite materials are increasing due to their high strength-to-weight ratio, excellent durability, good environmental resistance and design flexibility [1–3]. Recently, the application of FRP particularly, glass fibre reinforced polymer (GFRP) has been extended to civil construction such as bridge girders [4], bridge decks [5], space frame [6], retaining walls [7], railway sleepers [8–10] and other novel applications [11,12]. Those structures are often subjected to repetitive loading that causes degradation due to fibre fracturing, matrix cracking and fibre/matrix debonding [13]. Manalo et al. [14] further highlighted that the response of composite structures for a prolonged loading in time is critical as the design of FRP for civil infrastructure is normally governed by serviceability rather than strength. Thus, an in-depth understanding of the effect of repetitive loading on the structural performance of composites is needed to ensure they are safe for the targeted design life.

The behaviour of GFRP is linear and generally failed in brittle manner, which is fundamentally different from metals where failure initiates from a single crack and propagates until failure. Since the failure of GFRP is sudden without any warning, an understanding of their fatigue life with respect to the critical design parameters is important. The properties of the constituent materials, fibre orientations, applied stress level, stress concentration and frequency are the key parameters that can influence the fatigue life of GFRP materials [15]. The tension–tension fatigue behaviour of flax/epoxy composites having fibres in longitudinal, transverse and diagonal directions has exhibited a fatigue modulus loss of 10–55%, depending on the fibre orientations and loading level [16]. The study on fatigue damage growth behaviour of carbon fibre reinforced polymer composites indicated that the initiation and growth of the fatigue cracks are highly dependent on applied stress level and they observed the delamination and transverse crack propagation as the primary failure modes [17]. Gao's [18] study found that the high-strength material has great sensitivity to the notch effect (stress concentration) under fatigue loading. Researchers [16,19,20] claimed that the composite laminates generate heat at high frequency that affects the fatigue life of the material and therefore, they restricted the test frequency up to 4 Hz to avoid specimen self-heating. To predict the fatigue life,

* Corresponding author.
E-mail address: Wahid.Ferdous@usq.edu.au (W. Ferdous).
Peer review under responsibility of Karabuk University.

https://doi.org/10.1016/j.jestch.2020.01.001
2215-0986/

residual stiffness and strength, and failure mechanism, Shokrieh and Lessard [21,22] proposed a generalized residual material property degradation model. This model was able to explain the state of damage and predicted number of cycles to failure, but it required many experimental data for full material characterisation. Quaresimin et al. [13] considered the multiaxial fatigue criteria in predicting the fatigue life of composite laminates. They found a fair accuracy and largely unsafe predictions that emphasising the need of a deeper understanding of failure behaviour and establish a reliable predictive model. Understanding the effect of stress concentration and selecting a suitable fatigue failure criterion is important for predicting fatigue life.

The aforementioned review of literature has suggested that there is a knowledge gap in fatigue failure mechanism, their design considerations, reliable prediction of fatigue life and appropriate failure theory for GFRP laminates. More specifically, it is still remain questions (a) how the stress level dominated the failure mode, (b) how the loss of stiffness can be minimised when laminates are subjected to fatigue, (c) how important to avoid stress concentration in fatigue design, (d) is it possible to test the GFRP laminates at higher frequency (to reduce the testing time) than the traditional concept of testing at 4 Hz, (e) which failure criteria is the most appropriate to understand the failure behaviour of GFRP laminates and (f) how to improve the existing fatigue model for reliable prediction of fatigue life? The novelty of this study is to address these questions that contributed to the scientific knowledge for further understanding of the fatigue behaviour of composite structures. To achieve this goal, this study comprehensively (experimentally, analytically and numerically) investigated the effect of stress level, stress concentration, frequency and failure theory. The GFRP composite samples were tested at different stress levels (low to high) and frequencies (beyond the traditional concept) to understand the fatigue behaviour. Finite element analysis has been conducted to understand the effect of stress concentration on fatigue behaviour. Moreover, an analytical model has been suggested to predict the fatigue life of GFRP composites at different stress levels, frequencies and stress ratios. The outcome of this study is critical to understand the property retention and failure behaviour performance of composite materials under fatigue loading for simulating and designing structures subjected to moving loads, wind pressure and suction, and hydraulic forces.

2. Materials and method

2.1. GFRP composite laminates

The GFRP composite laminates used in this study were manufactured with stringent and consistent quality control using hand layup technique. The matrix used was a vinyl ester system and the bonded fibres improve surface quality and minimising the formation of resin-rich pockets by strictly controlling fibre alignments that provided stronger, stiffer and lightweight laminates. The burnout test in accordance with ASTM D2584 [23] revealed that the 10 equally thick fibre plies oriented in longitudinal (60%) and diagonal (40%) directions with a fibre volume ratio of 55%. The symmetric pattern of fabric created an orthogonal fibre composite. Rectangular-shaped specimens were cut from the composite plates using a water cooled diamond saw with a nominal dimensions of 300 mm × 25 mm × 5 mm including 50 mm tabs glued at both ends, leaving the specimens' gauge length of 200 mm.

2.2. Test setup

Static tensile tests were performed in accordance with ASTM-D3039 [24] in order to determine the ultimate tensile strength (UTS) and stiffness of the specimen. Five replicate samples were tested using servo-hydraulic MTS with a capacity of 100 kN at a crosshead speed of 1 mm/min. The specimen were carefully clamped onto the wedge jaws, which remain fixed in position on the test sample to prevent slipping at the gripping area and premature fracture. All the tests were conducted in normal room temperature (23 °C) and humidity (22%).

Fatigue tests were performed in tension–tension using the same computer-controlled servo-hydraulic MTS machine at different load amplitudes and frequencies in accordance with ISO 13,003 [25]. The chosen ranges of the loading level and loading frequency were from 0.25 to 0.80 UTS and 2 to 8 Hz, respectively [26]. To reduce the test time, higher frequency was used for high cycle fatigue tests. The ratio of minimum-to-maximum applied stresses in a cycle called as stress ratio (R) were constant to + 0.10 in order to apply tensile-tensile cyclic loads to the specimens. The load, displacement and time data were recorded at specified regular intervals during the fatigue tests. Tests have been stopped at specimens' failure or at eight million (8×10^6) cycles whichever comes first. For higher accuracy, two replicate samples were tested at each stress level in low cycle fatigue test as the initial trial shows the variation of results within 10%. The significant amount of time required to implement fatigue tests especially at higher cycles and the consistency of the previous results as well as the experiences of previous researcher [27] provided justification to test one sample at high cycles. The low applied stress for high cycle test is expected to distribute the stress more uniformly that lead to make the result consistent. All tests were carried out in the load control mode with a sinusoidal waveform of constant amplitude. The load scheme for fatigue test is shown in Fig. 1. Initially, the specimen was loaded gradually up to the middle of the minimum and maximum load levels and then cyclic load started with variable amplitude followed by constant amplitude after a few moments of stabilisation.

2.3. Finite element modelling

Three-dimensional finite element (FE) model was created using commercial ANSYS workbench software [28] in order to understand the fundamental fatigue behaviour of GFRP laminates. The reliability and accuracy of the analysis depends on material models, the size and type of the mesh, boundary conditions and edge preparation. The specimens were meshed using face meshing (usually more uniform, has less distorted elements, no triangles, and usually has less nodes) tool to obtain reliable results as this approach is suitable to avoid random meshing. Two different types of sample called as (a) sharp-edge and (b) round-edge were used in FE analysis. The shape, dimensions and meshing of the solid model are shown in Fig. 2.

Considering a good balance between solution time and the accuracy of results, a maximum element size of 2 mm was adopted in the model and the variation of properties in longitudinal and transverse directions were considered by modelling orthotropic material behaviour. The density and ultimate tensile strength of

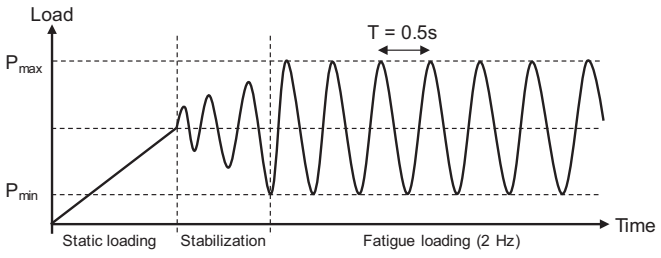

Fig. 1. Loading configuration for fatigue test.

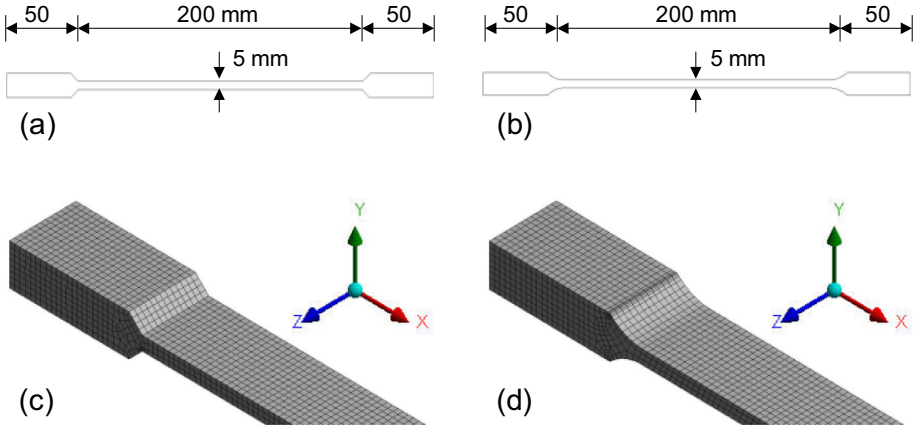

Fig. 2. Tensile specimens (a) sharp-edge specimen, (b) round-edge specimen, (c) meshing of sharp-edge specimen, and (d) meshing of round-edge specimen.

GFRP laminates were 2000 kg/m^3 and 500 MPa, respectively while the elastic modulus in longitudinal direction was 18 GPa. The transverse modulus, poisson's ratio and shear modulus were 9 GPa, 0.25 and 6 GPa, respectively as calculated based on the previously established relations between longitudinal and transverse properties [7,29]. Fixed support was considered in one end while the load was applied in other end of the specimen. Firstly, the model was verified with the static test results. The maximum stress criterion was considered to determine the static failure loads. Reference specimens were tested statically up to failure in longitudinal tensile direction, the results of which are reported in Fig. 3. This was used as the indication of the stress limits set in ANSYS for both static and fatigue investigation. The ultimate failure was noted when a significant part of the specimen exceeded the corresponding maximum stress limit. This criterion specifies the stress limit in different directions, providing a direct indication of critical stress component and potential failure mode. This failure criterion was preferred over other criterion (e.g., Tsai-Hill) because of the satisfactory description and the insightful indication of the failure modes. Once verified the model, a linear analysis was implemented for fatigue investigation. Eq. (10) was used to extract the wide range of stress versus cycle data (10% to 100% stress level) of the material required for fatigue analysis.

3. Results

3.1. Static test and verification of FE model

Before starting fatigue test, the tensile properties of the specimen was evaluated to determine the load corresponding to a particular stress level under cyclic loading. The representative tensile behaviour of the GFRP laminates is shown in Fig. 3(a) that indicates a linear elastic nature with brittle (sudden drop of load) mode of failure (Fig. 3b). The specimens were failed at an average load of 61 kN (CoV 6%) and 5.7 mm (CoV 3.7%) displacement that corresponds to an ultimate tensile strength of 500 MPa and strain of 0.028 with a tensile elastic modulus of 18 GPa. The FE model was verified by the experimental results. It can be seen that the FE model can capture the actual behaviour of the GFRP laminates in an acceptable manner (Fig. 3a). However, a high level of stress concentration (few elements reach up to 1229 MPa) was noticed at the tab for sharp-edge specimen (Fig. 3c) while the stresses were distributed quite uniformly (few elements reach up to a maximum of 529 MPa) for round-edge specimen (Fig. 3d). After verifying the FE model, it was then used for fatigue analysis.

3.2. Tension-tension fatigue test

The failure modes of the specimens are shown in Fig. 4(a). It can be seen that the specimens at 80% and 70% of the ultimate load were failed in tensile fracture of the fibres at the mid-height. However, when the specimens were subjected to 60%, 50% and 40% of the ultimate load, the failure occurred at the tab without scattered damage of the fibres (Fig. 4a). On the other hand, the specimens subjected to 25% of the ultimate load did not fail up to 8 million cycles and thereafter it was decided to stop the test. Therefore, it can be said that the stress concentration is another mode of fatigue failure and this type of failure is more likely occurred if there is a rapid change of cross sectional area or material properties and subjected to high number of fatigue cycles. The GFRP composite

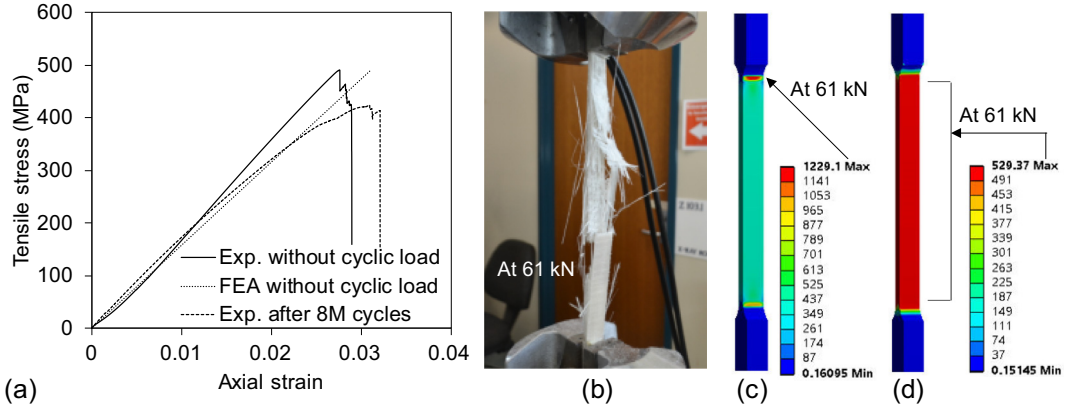

Fig. 3. Static test results (a) stress–strain plot, (b) failure of the specimen, (c) stress concentration in sharp-edge specimen, and (d) stress distribution in round-edge specimen.

Fig. 4. Failure modes under cyclic loading (a) for 40% to 80% stress level, and (b) test stopped at 8 million cycles for 25% stress level.

laminates used in this study is designed for an internal reinforcement of composite railway sleepers where only 3 million cycles are considered as a standard number for fatigue test [30]. However, the objective of this study is to understand the fatigue behaviour of the laminates for designing reinforcement of composite railway sleepers, therefore a fatigue test up to a very high number of cycles (i.e., 8 million) has been conducted. The slope of the load–displacement curve was decreased gradually indicating the loss of stiffness. The applied stresses, test frequency, average fatigue life (with standard deviation, SD), loss of stiffness and failure modes are provided in Table 1.

3.3. Damage

The surface of the GFRP specimen was examined using optical microscope at different stages of the fatigue test. Fig. 5 (a) shows the initial surface condition while the formation of micro-cracks after 3-million and 8-million cycles are illustrated in Fig. 5(b) and 5(c), respectively. It is obvious that the surface of the specimen was affected in scattered manner. This is because the GFRP composite laminate is inhomogeneous and anisotropic in nature and thus, the damage is generated at any location of the specimen according to the local stress distribution albeit in a random way, different from what generally happens along the crack propagation of metals [31–34]. Harris [35] indicated that the damage in fibre composite material may occur due to either independently or combined action of matrix cracking, fibre breakage, debonding and delamination. The outermost layer of the specimen was composed of longitudinal fibres and due to its greater elongation, the matrix attracted more stresses than fibres that generated cracks in the surface. This is further supported by the close observation of surface roughness that was captured by optical microscope and later analysed using image processing software as provided in Fig. 5 (d), 5(e) and 5(f). It can be seen that the surface of the specimen was sharp and flat at the beginning (Fig. 5d) whereas the sharpness and flatness decreased at 3-million cycles (Fig. 5e) and further deteriorated at 8-million cycles (Fig. 5f). As cycling continues, the viscoelastic deformations in the resin, but also growing of the micro-cracks, favour stress redistributions that causes cracks to propagate in transverse direction to some critical level when the stress reaches to the capacity, and ultimate failure of the specimen occur.

4. Modelling

The residual strength after constant amplitude of fatigue cycles is correlated to the initial static strength of the material [36]. The strength degradation of GFRP laminates is modelled based on the hypothesis that the material strength undergoes a continuous decay under cyclic loading and can be expressed by Eq. (1) using power law [37]. Under a constant frequency loading the strength degradation grows with the increase of fatigue cycles or time in other words. Therefore, Eq. (1) can be rewrite as a function of time domain and presented in Eq. (2).

$$\frac{d\sigma}{dn} = -C_1 n^{-m1} \tag{1}$$

$$\frac{d\sigma}{dt} = -C_2 t^{-m2} \tag{2}$$

In Eqs. (1) and (2), $\sigma$is the residual strength after n cycles; $t$is the time; C_1, C_2, $m1$and $m2$are the material constants. Here, Eq. (2) is based on the assumption that the temperature of the specimen will remain constant or close to constant during the test.

The material constant C_2 is the function of stress ratio (R), ultimate tensile strength (σ_u) and maximum applied stress (σ_{max}) that can be expressed by Eq. (3) where the constant A depends on the moisture content, temperature of the sample, material properties and loading type.

$$C_2 = A.F(R, \sigma_u, \sigma_{max}) \tag{3}$$

Sendeckyj [36] and Hertzberg and Manson [38] formulated the effect of R, σ_u and σ_{max} on the fatigue life of GFRP composites under tension–tension and fully reversed loading conditions as presented in Eq. (4).

$$F(R, \sigma_u, \sigma_{max}) = \sigma_u^{1-\gamma} \sigma_{max}^{\gamma} (1-\psi)^{\gamma} \tag{4}$$

Table 1
Fatigue test results.

Stress level (% UTS)	No. of samples	Frequency (Hz)	Average fatigue life (Cycles)	Stiffness loss (%)	Failure mode
80	2	2	360 (SD = 13)	3.74	Pure tension
70	2	2	984 (SD = 45)	5.77	Pure tension
60	2	2	1879 (SD = 92)	6.04	Stress concentration
50	2	2, 3, 4	29,174 (SD = 1503)	6.84	Stress concentration
40	1	2	187,292	7.45	Stress concentration
25	1	8	8,000,000	4.74	Did not fail (test stopped)

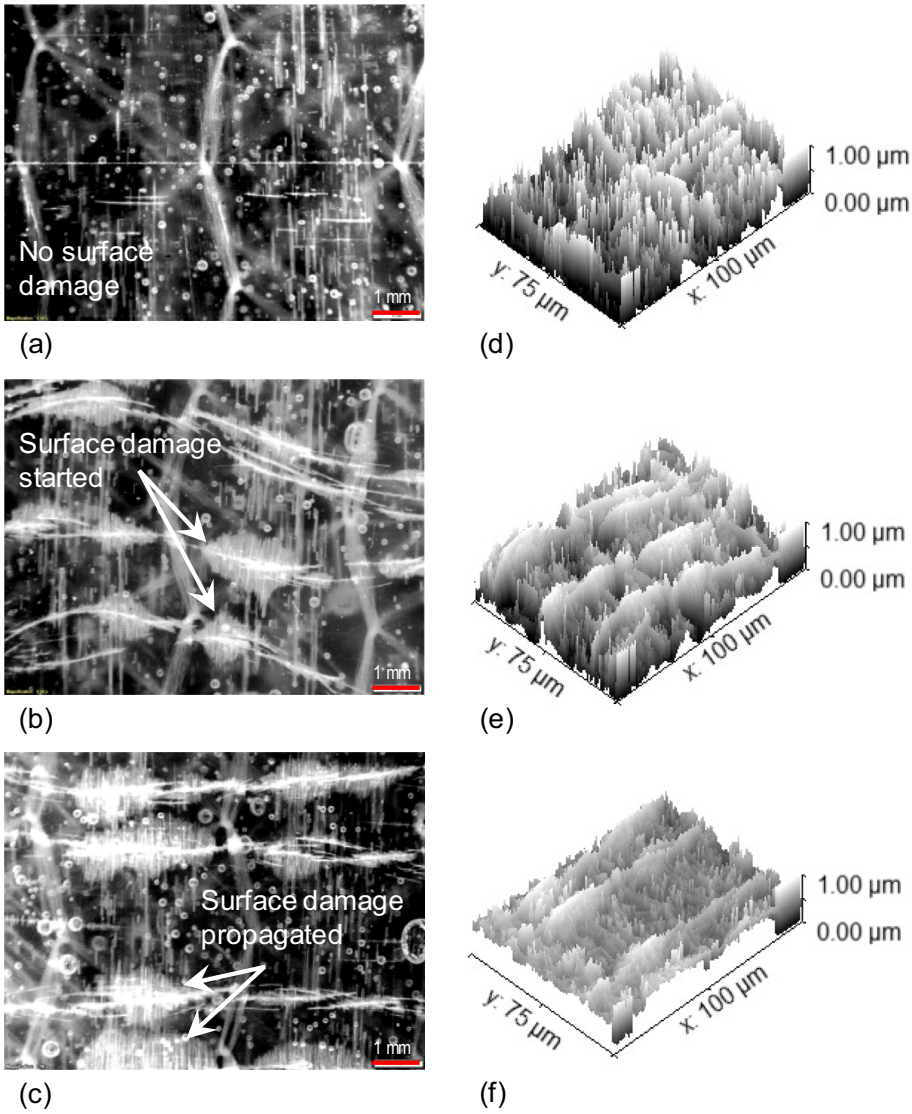

Fig. 5. Surface condition at (a) 0 cycle (beginning), (b) 3 million cycles (surface damage started) and (c) 8 million cycles (surface damage propagated); and surface roughness at (d) 0 cycle (beginning), (e) 3 million cycles and (f) 8 million cycles.

Hertzberg and Manson [38] experimentally determined the magnitude of constant γ in the range of $0.6 < \gamma < 7.6$ for fatigue damage propagation in composites. However, it can be calculated from the smallest angle (θ) between fibre direction and loading direction as given in Eq. (5).

$$\gamma = 1.6 - \psi sin\theta \tag{5}$$

In Eqs. (4) and (5), ψ is defined as

$\psi = R$ for $-\infty < R < 1$ (tension–tension and reverse loading)

$\psi = 1/R$ for $1 < R < \infty$ (compression-compression loading).

Fatigue failure will occur when the ultimate tensile strength (σ_u) decreases to be equal to the maximum applied stress(σ_{max}). The number of cycles required to degrade the strength of the material from σ_u toσ_{max} is the fatigue life. The fatigue life can be determined by integrating Eq. (2) from the beginning to the failure i.e., $t = t_0$ to $t = T$ as expressed in Eq. (6). The time (t) can be defined by the number of cycles (n) and frequency (f) as given in Eq. (7).

$$[\sigma]_{\sigma_u}^{\sigma_{max}} = -\frac{C_2}{-m_2+1}[t^{-m_2+1}]_{t=t_0,n=1}^{t=T,n=N} \tag{6}$$

$$t = \frac{n}{f} \tag{7}$$

Substituting Eq. (3), Eq. (4) and Eq. (7) in Eq. (6), the following relationship can be obtained

$$(\sigma_{max} - \sigma_u) = -\frac{A.\sigma_u^{1-\gamma}\sigma_{max}^{\gamma}(1-R)^{\gamma}}{-m_2+1}\frac{1}{f^{-m_2+1}}\left(N^{-m_2+1}-1\right) \tag{8}$$

Taking, $\alpha = \frac{A}{-m_2+1}$ and $\beta = -m_2 + 1$, the Eq. (8) can be rearranged as

$$\left(\frac{\sigma_u}{\sigma_{max}}-1\right)\left(\frac{\sigma_u}{\sigma_{max}}\right)^{\gamma-1}\frac{1}{(1-R)^{\gamma}} = \alpha(N^{\beta}-1)f^{-\beta} \tag{9}$$

Further rearranging Eq. (9), the fatigue life can be determined using Eq. (10).

$$N = \left[1+\frac{f^{\beta}}{\alpha}\left(\frac{\sigma_u}{\sigma_{max}}-1\right)\left(\frac{\sigma_u}{\sigma_{max}}\right)^{\gamma-1}\frac{1}{(1-R)^{\gamma}}\right]^{\frac{1}{\beta}} \tag{10}$$

The model presented in Eq. (9) has two parameters α and β that can be determined from few sets of experimental data. Only three straightforward fatigue test results at a particular stress ratio but different stress level are enough to determine the parameters α and β. Eq. (9) representing a straight line equation passing through

origin when plotting the left hand side of Eq. (9) against the quantity $(N^{\beta}-1)f^{-\beta}$. The best fit straight line can be obtained after several trials of β value (0.2589 for this study) where the slope of the straight line passing through origin is the value of α (0.1611 for this case).

The fatigue model presented in Eq. (10) considered the effect of stress ratio, applied maximum stress, frequency and material properties. The effect of frequency has not been considered in many existing fatigue models. For example, the model proposed by Caprino and D'Amore [37] did not consider the effect of frequency which is an important parameter that influence the fatigue life. Therefore, the model provided in this study has a clear advantage than the existing models [39,40]. The model presented in this study is not only restricted to the GFRP laminates but also suitable to predict fatigue life for any materials after adjusting the material constant parameters α and β.

5. Discussion

5.1. Effect of stress level

The effect of applied stress level on the fatigue life (cycles) is plotted in Fig. 6. The analytical model captured well the experimental behaviour and predicted fatigue life at very low stress level (i.e., at 20%). This figure shows that the fatigue life is increasing with the decrease of applied stress level, however, the response is slightly nonlinear even in semi-log plot. Previous researchers observed (comparison was made in normalised S-N curve) a linear variation of fatigue life in semi-log plot for carbon/epoxy, glass/epoxy, basalt/epoxy, carbon nanotube/epoxy and flax/epoxy fibre reinforced plastics [16,17,20,41]. The findings of this study indicates that the fatigue life of glass/vinyl ester increasing significantly for a small decrease of stress level, or in other words, the rate of increase of fatigue life for vinyl ester based composites is more than epoxy-based composites. Fig. 4(a) shows the failure of the specimen at different stress levels. It was observed that the specimens were failed in pure tension due to the rupture of fibres at 80% and 70% load. However, the failure occurred at the tab due to stress concentration when the specimens were subjected to a stress level of 60% or less. The stress concentrates slowly to a location where there is a change in sectional dimension or variation of material properties. The specimen fails in short period of time and at low number of cycles for a high level of applied stress (80% and 70%) that forced them to fail in pure tension. The variation in failure modes under cyclic load depends on fibre types and orientations, and agrees with the findings of Wu et al. [20] wherein they observed longitudinal and transverse cracking of fibres at failure.

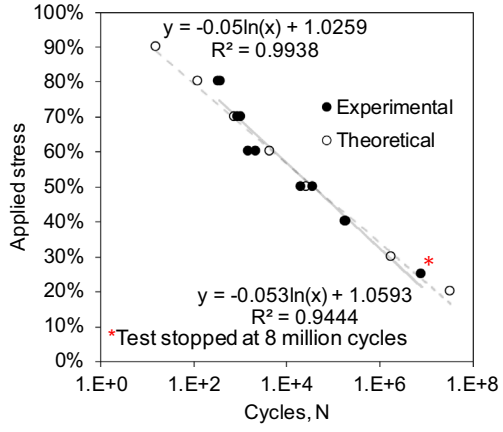

Fig. 6. Effect of stress level on fatigue life (S-N curve).

Fig. 7 plotted the initial and final hysteretic cycles of load–displacement curve for all levels of applied stress. Two major changes between first and last cycles are identified: (a) decrease of slope and (b) slight increase of area in the hysteretic cycle. The decrease of slope in load–displacement curve indicates the loss of stiffness of the specimen with the increase of fatigue cycles. The increase of fatigue cycle gradually transform the matrix softer and make the bond between resin and fibre weaker. The slight increase of area in last hysteretic cycle compare to the first indicates the dissipation of energy. The cumulative irreversible process of fatigue degradation occurs due to the internal friction and microfractures that reflects in different forms of dissipation mechanisms such as heat and mechanical hysteresis [42]. The potential energy converted into heat that rises the temperature of the specimen with the increase of fatigue cycles. It can be seen that the dissipated energy decreased as the applied load decreased, or in other words, the loss of energy per cycle increases with the increase of applied stress level. The narrow hysteresis loops gradually become straight lines as the applied load decreases.

Fig. 8 shows the residual stiffness at failure for different stress levels. It can be seen that the specimen lost their stiffness by 3.74%, 5.77%, 6.04%, 6.84% and 7.45% for 80%, 70%, 60%, 50% and 40% of the stress level, respectively. The specimen at 25% stress level did not fail up to 8 million cycles and the static test of the unbroken sample exhibited the strength up to 88% of its original as shown in Fig. 3(a). The tensile properties of composites are governed mainly by the fibres thus exhibited high strength and stiffness retention. In a similar GFRP composite, Vieira et al. [19], Manjunatha et al. [43] and Bourchak et al. [44] observed the loss of stiffness up to 20% at 40% stress level. Harris [35] indicated that the degradation of mechanical properties under cyclic loading largely depends on the lay-up of the composite and the mode of testing. The investigated laminates in the previous study [19,43,44] were composed of both longitudinal (0^{o}) and transverse (90^{o}) fibres while the laminates in the present study were fabricated without transverse fibres but having fibres in ± 45° directions which can retain better stiffness than transverse directional fibres. Therefore, it can be said that the loss of mechanical properties of laminated composites under cyclic loading can be minimised by avoiding fibres in transverse direction.

5.2. Effect of stress concentration

In reality, the structural components are often loaded with stress concentrating features such as tapers, notches, holes, flanges, grooves, embossments etc. that serves an essential purpose and cannot be eliminated. The abrupt change in section creates stress concentration and affects the overall performance of the structure. Using finite element modelling, Fig. 9 compares the fatigue performance of sharp-edge (high stress concentration) and round-edge (low stress concentration) specimens. It can be seen that the fatigue life (i.e., the number of cycles at failure) that is obtained for the same material is 40–80 times higher for round-edge specimen than sharp-edge at a particular stress level. Maragoni et al. [45] found that the fatigue damage initiation, evolution and stiffness drop are deeply affected by the stress concentrating features such as voids. Moreover, the effect of stress concentration on the fatigue life is more for higher than lower number of cycles. Therefore, a stress concentration factor need to be introduced to correlate the fatigue strength between sharp and round edge specimens. The simplified relationship is given in Eq. (11) while the stress concentration factor for the particular specimen in this study is proposed in Eq. (12). In Eq. (11), S_n is the adjusted fatigue strength for

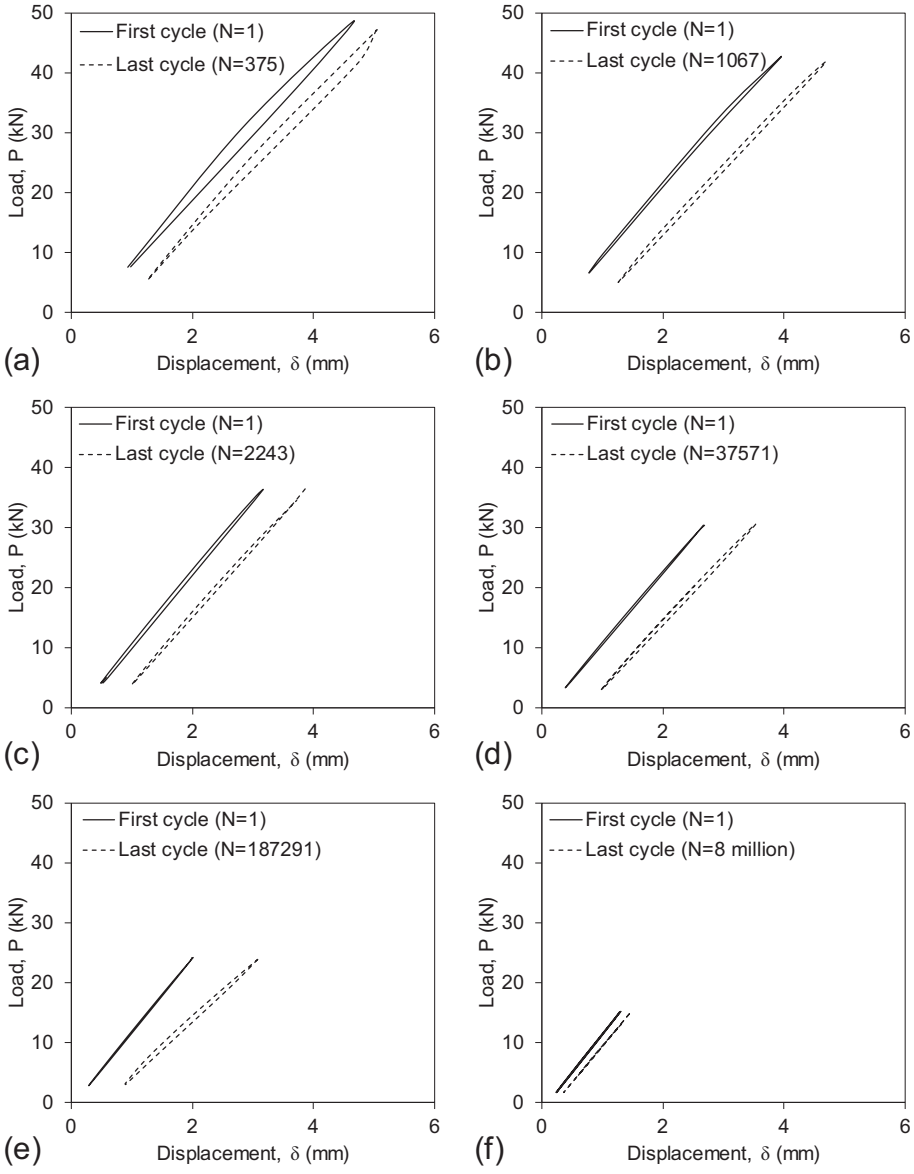

Fig. 7. Load-displacement behaviour at (a) 80%, (b) 70%, (c) 60%, (d) 50%, (e) 40% and (f) 25% of the ultimate load.

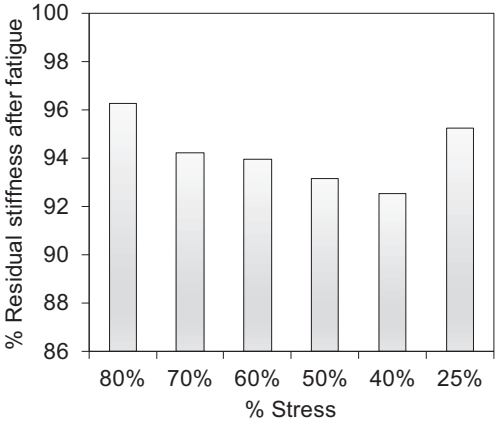

Fig. 8. Effect of stress level on stiffness (Note: the specimen did not fail at 25%).

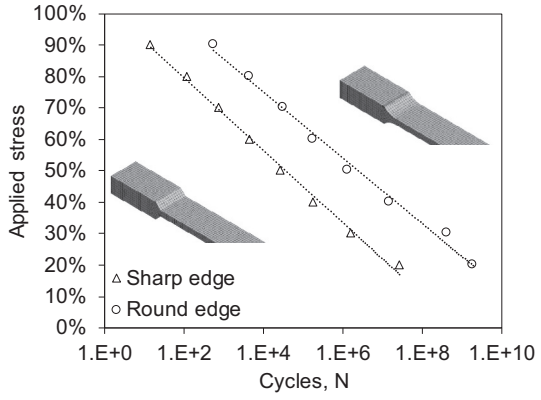

Fig. 9. Effect of edge preparation on fatigue life.

sharp-edge specimen while $S_n^{'}$ is the calculated fatigue strength for round-edge specimen assuming no stress concentration. The stress concentration factor (K_t) is dependent on the level of applied stress and can be determined using Eq. (12). An example, the S-N curve of GFRP material without stress concentration is given to the design engineer for determining maximum allowable stress for 1 million cycles of fatigue life where the structure need to be designed with sharp-edge specimen (i.e., components with stress concentration). Fig. 9 shows that the fatigue life of specimen without stress concentration (i.e., round-edge) is one million cycles when 53% of the ultimate load is applied. The stress concentration factor at this level of stress is 1.40, indicating that the maximum allowable stress need to be reduced to 38% for sharp-edge specimen to achieve one million cycles of fatigue life.

$$S_n = \frac{1}{K_t} S_n^{'} \tag{11}$$

$$K_t = \sqrt{\frac{\sigma_u}{\sigma_{max}}} \tag{12}$$

This study found that the stress concentration factor for sharp edge GFRP specimen can vary between 1 and 3, depending on the level of applied stress. This outcome supported the findings of Keller et al. [46] where they observed the tapered shape specimen (low stress concentration) performed better than the tabbed specimen (high stress concentration) under cyclic loading. Since the stress is much higher at the location of stress concentration, the fatigue failure generally initiate from this region. Therefore, when designing a structural component for cyclic loading, it is best to minimise stress concentration to prevent premature fatigue failure. This can be achieved by avoiding stress concentrating features from the design or by replacing sharp corners with the rounded fillets having radius as large as practically possible. In some cases where sharp corners are unavoidable, the stress concentration can be minimised by keeping this part away from the areas of peak stress under load.

5.3. Effect of frequency on heat generation

In fatigue test, it has been claimed that the specimen generates heat at high frequency and to avoid specimen self-heating, the test frequency is restricted up to 4 Hz [16,19,20]. This is more critical for fibre composites especially for resin/matrix interface as it can soften matrix with high temperature. Testing at low frequency however is time consuming for the high cycle fatigue test. The effect of loading frequency on heat generation has been investigated by measuring the surface temperature at the central height of the sample during fatigue experiment using laser temperature gun (non-contact infrared digital thermometer). The test was conducted under room temperature at a frequency of 2, 3, 4 and 8 Hz.

Fig. 10 plotted the variation of surface temperature with the increase of cycles at different frequencies. It can be seen that the surface temperature rises at the early stage of the fatigue test and stabilises after approximately 10,000 cycles. This is due to the surface smoothness of the specimen after 10,000 cycles as shown in Fig. 5 and the generation of micro-cracking that minimise friction between particles, resulting in a constant heat generation. The maximum increase of temperature recorded for 2, 3, 4 and 8 Hz frequencies are 6.8, 7.1, 6.2 and 7.9^{o}C, respectively, which indicates that the temperature can rise with the increase of frequency but its variation is not significant (1 ^{o}C) from 2 Hz to 8 Hz. According to ISO 13003 standard [25], the frequency should be selected in such a way that ensure a self-heating of the specimen remain below 10 ^{o}C during the test. The rise of temperature was obtained below 10 ^{o}C for all frequencies that indicates the

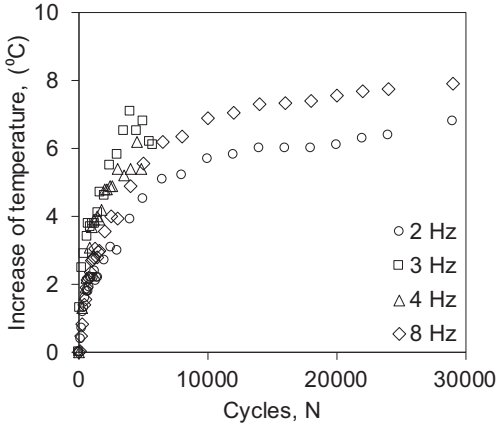

Fig. 10. Effect of frequency on surface temperature of the specimen.

GFRP sample can be tested at a frequency of 8 Hz without having influence of dynamic amplification because of internal friction. This finding can reduce the testing time by 50% compare to the traditional concept of testing at 4 Hz. The dissipation of energy during fatigue cycles produced heat that raised the temperature in the specimen and made the matrix soften that affecting the fibre–matrix interface and providing a slight decrease in the stiffness. It is worth noting that the findings are based on GFRP sample having low thermal conductivity, which is different from the metal where the heat can transfer quickly from one particle to another.

5.4. Failure theory

Failure theory is used to predict whether the stress at a critical point in an element of the specimen would result in failure. The common fatigue failure theories are Soderberg (Eq. (13)), Goodman (Eq. (14)), Gerber (Eq. (15)) and mean stress [18]. According to Goodman theory (Fig. 11a), a material is considered safe as long as the stress falls below the straight line that extends from the endurance limit (σ_e) on alternating stress (σ_a) axis to the ultimate tensile strength (σ_u) on mean stress (σ_m) axis. The Gerber theory (Fig. 11a) differs from the Goodman theory in that the failure line is parabolic that passes through the endurance limit and the ultimate tensile stress, hence less conservative (Fig. 11a). The Soderberg theory (Fig. 11a) is based on the yield strength (σ_y) of the material and more conservative than the previous two theories. The mean stress failure line is illustrated in Fig. 11(b) for different loading types. Mean stress theory is particularly important when stress-cycle (S-N) curve is defined with different stress ratios (i.e., R-values). The finite element software accounts for the mean stress by linear interpolation between the curves for a different R-value. The question now arises which failure theory is the most appropriate for GFRP material?

$$\text{SoderbergEq.}\ \frac{\sigma_a}{\sigma_e} + \frac{\sigma_m}{\sigma_y} = 1 \tag{13}$$

$$\text{GoodmanEq.}\ \frac{\sigma_a}{\sigma_e} + \frac{\sigma_m}{\sigma_u} = 1 \tag{14}$$

$$\text{GerberEq.}\ \frac{\sigma_a}{\sigma_e} + \left(\frac{\sigma_m}{\sigma_u}\right)^2 = 1 \tag{15}$$

As mentioned, the Soderberg failure criteria is based on the yield strength of the material, hence, this theory is not appropriate for a material like GFRP where there is no yield point. To understand the most appropriate failure theory for GFRP material, Fig. 12(a) plotted the fatigue sensitivity response using different

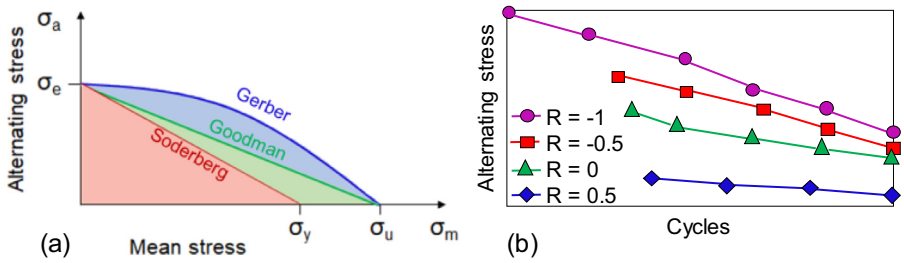

Fig. 11. Fatigue failure theory (a) Gerber, Goodman and Soderberg, and (b) Mean stress.

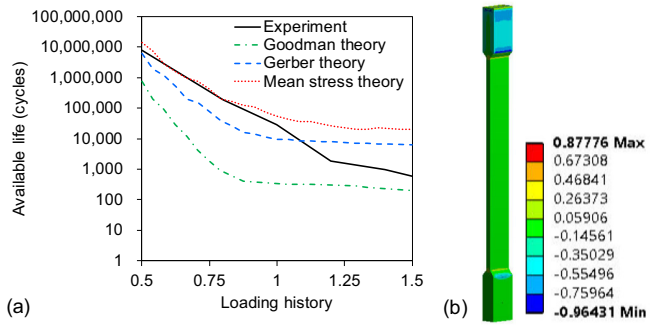

Fig. 12. Effect of failure theory (a) fatigue sensitivity, and (b) biaxiality indication.

failure theories and compares with the experimental results. The fatigue sensitivity results were obtained from FE analysis at an applied stress of 50% to the ultimate that corresponds to the loading history of 1. It can be seen that the mean stress theory closely captured the experimental behaviour for an applied stress between 25% (loading history 0.5) and 50% (loading history 1) of the ultimate strength as the mean stress curve closely following the experimental results in this region. On the other hand, the Goodman failure theory is the most appropriate when high level of stress is applied i.e., 60% (loading history 1.2) and above. Fig. 4(a) shows that the specimens at high stress level failed in pure tension due to fibre fracture (brittle failure) for which a criteria with linear variation of ultimate and endurance strength (Goodman theory) is expected to perform better. The reliability of the FE results in Fig. 12(a) is further verified by observing the biaxiality indication of the specimen as shown in Fig. 12(b). A biaxiality of zero (or close to) in the span of the specimen ensures the uniaxial stress was developed.

6. Conclusions

This study investigated the axial tension–tension fatigue behaviour of GFRP composite laminates. The effect of stress level, stress concentration and frequency on the fatigue life of the material were studied through experimental, analytical and finite element modelling from which the following conclusions are drawn:

- The stress levels affected the failure behaviour of GFRP composites. Specimens failed in pure tension due to the rupture of longitudinal fibres for an applied stress of 70% of the ultimate tensile strength or more while the failure occurred due to stress concentration when subjected to a stress of 60% of the ultimate tensile strength or less.
- The vinyl ester-based laminated composites exhibited 88% retention of its original strength after 8 million cycles of fatigue. The loss of stiffness of the laminated composites can be minimised by avoiding fibres in transverse direction.
- Stress concentration reduced the fatigue life of laminated composites and the detrimental effect increased at high number of cycles. Depending on the applied stress level, a stress concentration factor from 1 to 3 has been proposed to correlate the fatigue strength between sharp and round edge GFRP composites. Stress concentrating features should be avoided from the design for improving fatigue life of the composites.
- Increasing test frequency from 2 Hz to 8 Hz raised the self-heating temperature only by 1 °C (from 6.8 °C to 7.9 °C) and remained below the maximum allowable of 10 °C for both cases. Therefore, GFRP composites can be tested at a frequency of 8 Hz without having influence of dynamic amplification as a result of internal friction. This finding can reduce the testing time by 50% compare to the traditional concept of testing GFRP composites at 4 Hz frequency.
- Mean stress failure criteria is the most appropriate for GFRP composites under low stress condition (50% of the ultimate strength or less) while the Goodman failure criteria obtained suitable if the specimen is subjected to high stress (60% of the ultimate strength or more).
- The analytical model used in this study has taken into account the effect of stress ratio, applied maximum stress, frequency and material properties that is able to predict reliably the fatigue life of GFRP composites even at very high cycles.

Acknowledgements

This project is supported by the Cooperative Research Centres Projects (CRC-P57360 - CRC-P Round 3) grants. The authors gratefully acknowledge the material support from the Austrak Pty Ltd.

Declaration of interests

The authors declare that they have no known competing financial interests or personal relationships that could have appeared to influence the work reported in this paper.

References

[1] C.E. Bakis, L.C. Bank, V.L. Brown, E. Cosenza, J.F. Davalos, J.J. Lesko, et al., Fiber-reinforced polymer composites for construction — State-of-the-art review, J. Compos. Constr. 6 (2002) 73–87.
[2] W. Ferdous, T.D. Ngo, K.T.Q. Nguyen, A. Ghazlan, P. Mendis, A. Manalo, Effect of fire-retardant ceram powder on the properties of phenolic-based GFRP composites, Compos. B Eng. 155 (2018) 414–424.
[3] W. Ferdous, A. Manalo, T. Aravinthan, Effect of beam orientation on the static behaviour of phenolic core sandwich composites with different shear span-to-depth ratios, Compos. Struct. 168 (2017) 292–304.
[4] Keller T, Gürtler H. Composite action and adhesive bond between fiber-reinforced polymer bridge decks and main girders. Journal of composites for construction. 2005;9.
[5] S. Yanes-Armas, Jd. Castro, T. Keller, System transverse in-plane shear stiffness of pultruded GFRP bridge decks, Eng. Struct. 107 (2016) 34–46.
[6] X. Yang, Y. Bai, F.J. Luo, X.-L. Zhao, F. Ding, Dynamic and fatigue performances of a large-scale space frame assembled using pultruded GFRP composites, Compos. Struct. 138 (2016) 227–236.

[7] W. Ferdous, Y. Bai, A.D. Almutairi, S. Satasivam, J. Jeske, Modular assembly of water-retaining walls using GFRP hollow profiles: Components and connection performance, Compos. Struct. 194 (2018) 1–11.
[8] W. Ferdous, A. Manalo, G. Van Erp, T. Aravinthan, K. Ghabraie, Evaluation of an innovative composite railway sleeper for a narrow-gauge track under static load, J. Compos. Constr. 22 (2018) 1–13.
[9] G. Koller, FFU synthetic sleeper – Projects in Europe, Constr. Build. Mater. 92 (2015) 43–50.
[10] W. Ferdous, A. Manalo, T. Aravinthan, A. Fam, Flexural and shear behaviour of layered sandwich beams, Constr. Build. Mater. 173 (2018) 429–442.
[11] H. Fang, Y. Bai, W. Liu, Y. Qi, J. Wang, Connections and structural applications of fibre reinforced polymer composites for civil infrastructure in aggressive environments, Compos. B Eng. 164 (2019) 129–143.
[12] W. Ferdous, Effect of beam-column joint stiffness on the design of beams, in: S. T. Smith (Ed.), 23rd Australasian Conference on the Mechanics of Structures and Materials (ACMSM23), Southern Cross University, Byron Bay, Australia, 2014, pp. 701–706.
[13] M. Quaresimin, L. Susmel, R. Talreja, Fatigue behaviour and life assessment of composite laminates under multiaxial loadings, Int. J. Fatigue 32 (2010) 2–16.
[14] A. Manalo, T. Aravinthan, A. Fam, B. Benmokrane, State-of-the-art review on FRP sandwich systems for lightweight civil infrastructure, J. Compos. Constr. 21 (2016) 1–16.
[15] T. Tanimoto, S. Amijima, Progressive nature of fatigue damage of glass fiber reinforced plastics, J. Compos. Mater. 9 (1975) 380–390.
[16] S. Liang, P.-B. Gning, L. Guillaumat, Properties evolution of flax/epoxy composites under fatigue loading, Int. J. Fatigue 63 (2014) 36–45.
[17] A. Hosoi, N. Sato, Y. Kusumoto, K. Fujiwara, H. Kawada, High-cycle fatigue characteristics of quasi-isotropic CFRP laminates over 10^8 cycles (Initiation and propagation of delamination considering interaction with transverse cracks), Int. J. Fatigue 32 (2010) 29–36.
[18] Y. Gao, Fatigue stress concentration sensitivity and stress ratio effect of a 40CrNi2Si2MoVA steel, Mater. Lett. 186 (2017) 235–238.
[19] P.R. Vieira, E.M.L. Carvalho, J.D. Vieira, R.D. Filho, Experimental fatigue behavior of pultruded glass fibre reinforced polymer composite materials, Compos. B Eng. 146 (2018) 69–75.
[20] Z. Wu, X. Wang, K. Iwashita, T. Sasaki, Y. Hamaguchi, Tensile fatigue behaviour of FRP and hybrid FRP sheets, Compos. B Eng. 41 (2010) 396–402.
[21] M.M. Shokrieh, L.B. Lessard, Progressive fatigue damage modeling of composite materials, Part I: Modeling, J. Compos. Mater. 34 (2000) 1056–1080.
[22] M.M. Shokrieh, L.B. Lessard, Progressive fatigue damage modeling of composite materials, Part II: Material characterization and model verification, J. Compos. Mater. 34 (2000) 1081–1116.
[23] ASTM-D2584. Standard test method for ignition loss of cured reinforced resins. West Conshohocken, PA: ASTM International; 2018.
[24] ASTM-D3039. Standard test method for tensile properties of polymer matrix composite materials. USA: ASTM International; 2017.
[25] ISO-13003. Fibre-reinforced plastics - Determination of fatigue properties under cyclic loading conditions. International Organization for Standardization; 2003.
[26] Wu C, Feng P, Bai Y. Comparative study on static and fatigue performances of pultruded GFRP joints using ordinary and blind bolts. Journal of composites for construction. 2015;19.
[27] Y. Ochi, K. Masaki, T. Matsumura, T. Sekino, Effect of shot-peening treatment on high cycle fatigue property of ductile cast iron, Int. J. Fatigue 23 (2001) 441–448.
[28] ANSYS. Introduction to ANSYS Workbench. www.ansys.com; 2017. p. 1-11.
[29] W. Ferdous, A.D. Almutairi, Y. Huang, Y. Bai, Short-term flexural behaviour of concrete filled pultruded GFRP cellular and tubular sections with pin-eye connections for modular retaining wall construction, Compos. Struct. 206 (2018) 1–10.
[30] W. Ferdous, A. Manalo, G. Van Erp, T. Aravinthan, S. Kaewunruen, A. Remennikov, Composite railway sleepers – Recent developments, challenges and future prospects, Compos. Struct. 134 (2015) 158–168.
[31] B. Denkena, C. Schmidt, K. Völtzer, T. Hocke, Thermographic online monitoring system for Automated Fiber Placement processes, Compos. B Eng. 97 (2016) 239–243.
[32] T. Lisle, C. Bouvet, M.L. Pastor, P. Margueres, R.P. Corral, Damage analysis and fracture toughness evaluation in a thin woven composite laminate under static tension using infrared thermography, Compos. A Appl. Sci. Manuf. 53 (2013) 75–87.
[33] W. Harizi, S. Chaki, G. Bourse, M. Ourak, Mechanical damage assessment of Glass Fiber-Reinforced Polymer composites using passive infrared thermography, Compos. B Eng. 59 (2014) 74–79.
[34] D. Palumbo, R.D. Finis, P.G. Demelio, U. Galietti, A new rapid thermographic method to assess the fatigue limit in GFRP composites, Compos. B Eng. 103 (2016) 60–67.
[35] B. Harris, A historical review of the fatigue behaviour of fibre-reinforced plastics. Fatigue in Composites: Science and Technology of the Fatigue Response of Fibre-Reinforced Plastics, Woodhead Publishing, 2003.
[36] Sendeckyj GP. Chapter 10 - Life Prediction for Resin-Matrix Composite Materials. Composite Materials Series1991. p. 431-83.
[37] G. Caprino, A. D'Amore, Flexural fatigue behaviour of random continuous-fibre-reinforced thermoplastic composites, Compos. Sci. Technol. 58 (1998) 957–965.
[38] R.W. Hertzberg, J.A. Manson, Fatigue of engineering plastics, Academic Press, 1980.
[39] J. Huang, M.L. Pastor, C. Garnier, X.J. Gong, A new model for fatigue life prediction based on infrared thermography and degradation process for CFRP composite laminates, Int. J. Fatigue 120 (2019) 87–95.
[40] J. Degrieck, W.V. Paepegem, Fatigue damage modeling of fibre-reinforced composite materials: Review, Appl. Mech. Rev. 54 (2001) 279–300.
[41] Y.-M. Jen, Y.-C. Wang, Stress concentration effect on the fatigue properties of carbon nanotube/epoxy composites, Compos. B Eng. 43 (2012) 1687–1694.
[42] A. Kahirdeh, M.M. Khonsari, Energy dissipation in the course of the fatigue degradation: Mathematical derivation and experimental quantification, Int. J. Solids Struct. 77 (2015) 74–85.
[43] C.M. Manjunatha, A.C. Taylor, A.J. Kinloch, S. Sprenger, The tensile fatigue behavior of a GFRP composite with rubber particle modified epoxy matrix, J. Reinf. Plast. Compos. 29 (2010) 2170–2183.
[44] M. Bourchak, A. Algarni, A. Khan, U. Khashaba, Effect of SWCNTs and graphene on the fatigue behavior of antisymmetric GFRP laminate, Compos. Sci. Technol. 167 (2018) 164–173.
[45] L. Maragoni, P.A. Carraro, M. Peron, M. Quaresimin, Fatigue behaviour of glass/epoxy laminates in the presence of voids, Int. J. Fatigue 95 (2017) 18–28.
[46] T. Keller, T. Tirelli, A. Zhou, Tensile fatigue performance of pultruded glass fiber reinforced polymer profiles, Compos. Struct. 68 (2005) 235–245.